DOI: 10.17650/1683-3295-2023-25-3-43-58

Original report

SURGICAL ASPECTS OF CLASSIFICATION AND NEUROIMAGING CHARACTERISTICS OF IDIOPATHIC HYDROCEPHALUS IN ADULTS

K.V. Shevchenko, V.N. Shimansky, S.V. Tanyashin, V.K. Poshataev, V.V. Karnaukhov, M.V. Kolycheva, K.D. Solozhentseva, Yu.V. Strunina

N.N. Burdenko National Medical Research Center of Neurosurgery, Ministry of Health of Russia; 16 4th Tverskaya-Yamskaya St., Moscow 125047, Russia

Contacts: Kirill Viktorovich Shevchenko *kshevchenko@nsi.ru*

Background. Hydrocephalus can be developing by a traumatic brain injury, intracranial hemorrhage, tumor, meningitis of congenital malformation of the central nervous system. When the cause of the hydrocephalus is unclear, it is supposed as idiopathic hydrocephalus. The most important classification features are the etiology and level of CSF obstruction. The classification was improved and developed with diagnostic and surgical methods simultaneously. Currently, the neurosurgeons have the possibility for usage of various methods and techniques of surgical treatment with their advantages and disadvantages. Systematization of radiological parameters is necessary to make a decision about the type of the surgery.

Aim. to analyze and systematize the neuroimaging characteristics of various forms of idiopathic hydrocephalus in adults, to assess the possible classification of idiopathic hydrocephalus.

Materials and methods. Between October 2011 and March 2021 290 patients with idiopathic adult hydrocephalus were operated at the N.N. Burdenko National Medical Research Center of Neurosurgery of the Ministry of Health of Russia: onset of symptoms in adulthood; no indications of the etiology of hydrocephalus and congenital hydrocephalus. The age of the patients was 50 ± 18.2 (18–85) years. The magnetic resonance images of patients were evaluated for the size of the ventricles, condition of convexital and basal subarachnoid spaces, obstruction of the CSF pathways, and changes in the position of the premamillary membrane, septum pellucidum, the roof of the 3rd ventricle and the tonsils of the cerebellum, the size of the sella turcica, the angle of the corpus callosum. The frequency of each of these parameters is statistically estimated for each form of idiopathic hydrocephalus.

Results. Aqueduct stenosis has become the most frequent form of idiopathic hydrocephalus. Hydrocephalus in obstruction of the foramen of Monroe, aqueduct, foramen of Magendie, and cisterns of the posterior cranial fossa was significantly more characteristic of young people (p <0.05). Hydrocephalus with obstruction of convexital CSF spaces can be called hydrocephalus of the elderly (p <0.001). Hydrocephalus without verified signs of occlusion CSF pathways occurs equally in all age groups. The FOHR index was significantly more important, and only in case of cisternal obstruction. Enlargement one or both lateral ventricles and flattening of the roof of the 3rd ventricle is characterized for Monro's foramen obstruction (p <0.001). The membrane at the outlet of the 4th ventricle and the absence of the "flow void" was typically only for patients with obstruction of the foramen of Magendie (p <0.001). Ventral dislocation of the premamillary membrane was characteristic of obstruction of the cerebral aqueduct, the foramen of Magendie, and cisterns of the posterior cranial fossa. Compression of the convexital CSF spaces occurred in case of obstruction of the aqueduct, the foramen of Magendie, but CSF spaces of the posterior cranial fossa – only with obstruction of the foramen of Magendie. Dilation of the 4th ventricle was significantly associated with obstruction of the foramen of Magendie and cisterns of the posterior cranial fossa (p <0.05). DESH symptom was significantly associated with obstruction of convexital CSF spaces (p <0.001). Additional membranes in the cisterns of the posterior fossa were found only in cases of cisternal obstruction (p <0.001). Cerebellar tonsils herniation was observed with obstruction of the foramen of Monroe, cerebral aqueduct, and foramina of Magendie.

Conclusion. Because of statistical analysis, general signs found in all types of hydrocephalus, and private ones, characterizing only specific signs of the type of the disease, both were found. The classification is logical and justified, it is well applicable in neurosurgical and radiological practice. It allows rational planning of diagnostic evaluation and treatment of patients. A modern magnetic resonance imaging protocol should include T2 scans (with "flow void") and FIESTA/CISS scans in the required planes, axial FLAIR scans.

Keywords: hydrocephalus, idiopathic adult hydrocephalus, classification of hydrocephalus, occlusive hydrocephalus, obstructive hydrocephalus, foramen of Monroe, aqueduct of brain, foramen of Magendie, normal pressure hydrocephalus, arachnoid cistern, endoscopic third ventriculostomy, ventriculoperitoneal shunt

Original report

For citation: Shevchenko K.V., Shimansky V.N., Tanyashin S.V. et al. Surgical aspects of classification and neuroimaging characteristics of idiopathic hydrocephalus in adults. Neyrokhirurgiya = Russian Journal of Neurosurgery 2023;25(3): 43–58. (In Russ.). DOI: 10.17650/1683-3295-2023-25-3-43-58

BACKGROUND

Hydrocephalus is an enlargement of the cerebral ventricles due to abnormal cerebrospinal fluid (CSF) circulation [1, 2]. Hydrocephalus can be caused by traumatic brain injury, subarachnoid hemorrhage, tumor, neonatal intraventricular hemorrhage, infectious inflammation of the cerebral dura mater, developmental defects of the nervous system. Symptomatic hydrocephalus without the obvious cause is called idiopathic hydrocephalus [1].

Hydrocephalus classification allows determining the indications and selecting the method of surgical treatment. The most important classifying characteristics of hydrocephalus are disease etiology and the level of CSF flow obstruction [2].

Hydrocephalus classification has been changing and developing in parallel with development and implementation of new diagnostic and treatment techniques. In 1919, W.E. Dandy identified the choroid plexus of the lateral ventricles as the main structure producing CSF. Evaluating the possibility of injected contrast agent diffusing from the cerebral ventricles into the spinal subarachnoid space (SSS), he identified "communicating" and "non-communicating" hydrocephalus [3]. In 1960, J. Ransohoff et al. were the first to prove that CSF flow can be obstructed both in the ventricular system of the brain and outside it. They proposed the term "extraventricular obstructive hydrocephalus" signifying CSF flow obstruction outside the ventricles. In contrast, they called intraventricular obstruction "intraventricular obstructive hydrocephalus" [2, 4]. J. Li et al. injected kaolin protein into the arachnoid cisterns of the posterior cranial fossa (PCF) in test animals and showed the possibility of hydrocephalus development in isolated obstruction of PCF ventral cisterns and in isolated obstruction of convexital SSS [5].

Magnetic resonance imaging (MRI) of the head is the main method of hydrocephalus diagnosis. It allows to ascertain the conductivity of the cerebral aqueduct (CA) through sequences of CSF flow-sensitive modes [6–8]. Sagittal sections show the position of the premamillar membrane (PMM) dividing the third ventricle and the interpeduncular cistern. It is assumed that its prolapse in the ventral direction corresponds to the presence of constant pressure gradient between these two CSF-containing spaces and, therefore, indirectly points to CSF flow obstruction. This sign reliably predicts the possibility of effective endoscopic third ventriculostomy [9]. Additionally, MRI allows to identify cases of PMM ventral dislocation without intraventricular CSF flow obstruction [10, 11].

In 1998, H. Kitagaki et al. used volumetric MRI in idiopathic normal-pressure hydrocephalus and described extension of the Sylvian fissures and isolated sulci on the convexital surface of the cerebral hemispheres with simultaneous SSS compression in the area of the superior sagittal sinus and in the longitudinal fissure [12]. Later, this condition was named disproportionately enlarged subarachnoid space hydrocephalus (DESH), and the SYNPHONI trial confirmed high prognostic value of this symptom in diagnosis of idiopathic normal-pressure hydrocephalus [13, 14].

There is no classification of idiopathic hydrocephalus in the current scientific literature. Idiopathic normal-pressure hydrocephalus and idiopathic aqueductal stenosis are considered separate conditions. Additionally, detailed search and analysis of the publications confirm high variability of the diagnosis. Systematization of neuroradiological signs and focus on the key visualization characteristics are absent for various forms of idiopathic hydrocephalus which complicates diagnosis and, therefore, adequate patient management and treatment. Classification and systematization of various forms of the disorder are necessary due to development of endoscopic techniques, new treatment methods.

Aim is to analyze and systematize neuroimaging characteristics of various forms of adult idiopathic hydrocephalus (AIH), evaluate its possible classification.

MATERIALS AND METHODS

Between October of 2011 and March of 2021 at the N.N. Burdenko National Medical Research Center for Neurosurgery (hereafter Neurosurgery Center), 290 patients underwent treatment due to signs of a disorder corresponding to AIH criteria:

- symptoms appearing in adult age;
- absence of indicators of hydrocephalus etiology and congenital hydrocephalus.

Additionally, the study included patients who previously did not receive surgical treatment due to hydrocephalus outside of the Neurosurgery Center. The database has been prospectively updated during the whole period of material accumulation.

Patient age varied between 18 and 85 years (mean age was 50 ± 18.2 years). There were more women in the total group (54.1 %).

In September of 2014 at the annual conference of the International Society for Hydrocephalus and CSF Disorders (ISHCSF), radiologist Ari Blitz proposed a classification of adult hydrocephalus per the level of CSF flow obstruction (Table 1). It was based on the approach proposed earlier by H.L. Rekate [2]. Based on evaluation of the neuroradiological parameters presented below, the patients were divided into groups depending on the obstruction level per the Blitz's classification.

Table 1. *Classification of idiopathic hydrocephalus of adults*

Type of hydrocephalus	Name of hydrocephalus	Place of obstruction
AH1	Hydrocephalus due to foramen of Monroe obstruction (fig. 1, 2)	Foramen of Monroe
AH2a	Hydrocephalus due to aqueduct stenosis (fig. 3)	Aqueduct of the brain
AH2b	Hydrocephalus due to foramen of Magendie and Lushka obstruction (fig. 4)	Foramen of Magendie and Lushka
AH3	Hydrocephalus due to obstruction of the posterior cranial fossa cisterns (fig. 5)	Posterior cranial fossa cisterns
AH4	Hydrocephalus with disproportional enlarged subarachnoid spaces (fig. 6)	Convexital subarachnoid spaces
AH5	Hydrocephalus without CSF obstruction (fig. 7)	Absence of obstruction (this wasn't found)

Note. *Here and in table 2, 3: AH – adult hydrocephalus.*

The data of MRI performed during patients admission at the Neurosurgery Center were analyzed in the context of the condition of various parts of the CSF fluid pathways and changes in the position of anatomical structures.

The lateral ventricles were considered enlarged if the frontal occipital horn ratio (FOHR) was ≥0.4 [15] or the Evans index was >0.29.

CA obstruction was diagnosed if the lateral and 3rd ventricles were enlarged and:

- visible membranes were present in the CA lumen in FIESTA sagittal images;
- CA lumen had stenosis by thickened quadrigeminal plate;
- CSF flow was absent in the CA per images obtained in CFS flow-sensitive modes (T2 3DCUBE, phase contrast MRI (PC-MRI));
- CSF hyperpulsation was observed in PC-MRI in combination with CSF pulsation artifact in CA;
- ventral dislocation of PMM was observed. This sign was evaluated per sagittal MRI sections, preferably in magnetic resonance (MR) cisternography mode. If the available images did not allow to assess PMM dislocation, this sign was considered to be absent, and patients were sent to additional examinations. Normal PMM position was stated in cases when it was located on the line connecting mammillary bodies and the optic chiasm.

Conductivity at the exit from the 4th ventricle was evaluated similarly. Additionally, to the described signs, tetraventricular hydrocephalus was also assessed in all cases.

Convexital SSS were considered compromised if T2 MRI did not allow to visualize CSF above the gyri; in other cases, they were considered visible, or DESH symptom was present (see below).

Disproportional SSS extension (DESH) was assessed as SSS compression in the posterior parts of the longitudinal fissure and near the posterior third of the superior sagittal sinus in combination with widened lateral sulci and, sometimes, sulci on the convexital surface of the cerebral hemispheres.

The 3rd ventricle was considered enlarged at 3rd ventricle transverse width >0.048; 4th ventricle was considered enlarged at 4th ventricle transverse width (FVWT) >0.14 and/or 4th ventricle anteroposterior width (FVWAP) >11.91 mm.

PCF subarachnoid spaces were evaluated visually without the use of objective parameters. The evaluation was based on the CSF signal on the medial sagittal images, their conductance was assessed by the presence of CSF pulsation artifact.

The presence of leukoaraiosis was assessed in T2/FLAIR MRI, as well as changes in the signal from the basal ganglia, white matter.

The sella turcica was considered enlarged for anteroposterior diameter >15 mm, depth >13 mm.

The cerebral aqueduct was considered normal in the absence of 3rd ventricle enlargement and presence of CSF pulsation artifact in it. The following types of CA condition were identified: enlarged rostrally (in case of frontal part enlargement); enlarged caudally (in case of distal part enlargement); enlarged whole CA; CA stenosis (combination of triventricular hydrocephalus, presence of CSF pulsation artifact in the CA, and CSF hyperpulsation in the CA per PC-MRI).

Cisterna magna size was evaluated subjectively. Its filling with the cerebellar tonsils, CSF signal visualization and pulsation were taken into account.

Conductance of the PCF basal cisterns along the ventral surface of the brainstem was evaluated by the presence of CSF pulsation artifact in T2-weighted MRI. FIESTA (CISS) MRI was used to visualize the presence of additional membranes in the PCF cistern space.

Cerebellar tonsils were considered displaced if their margin was lower than the McRae line.

For identification of more specific signs in each group per the Blitz's classification, study group patient data were compared to the data from the rest of the patients. For comparison of frequency of occurrence of qualitative signs, Fisher's exact test (two-sided variant) was used. For

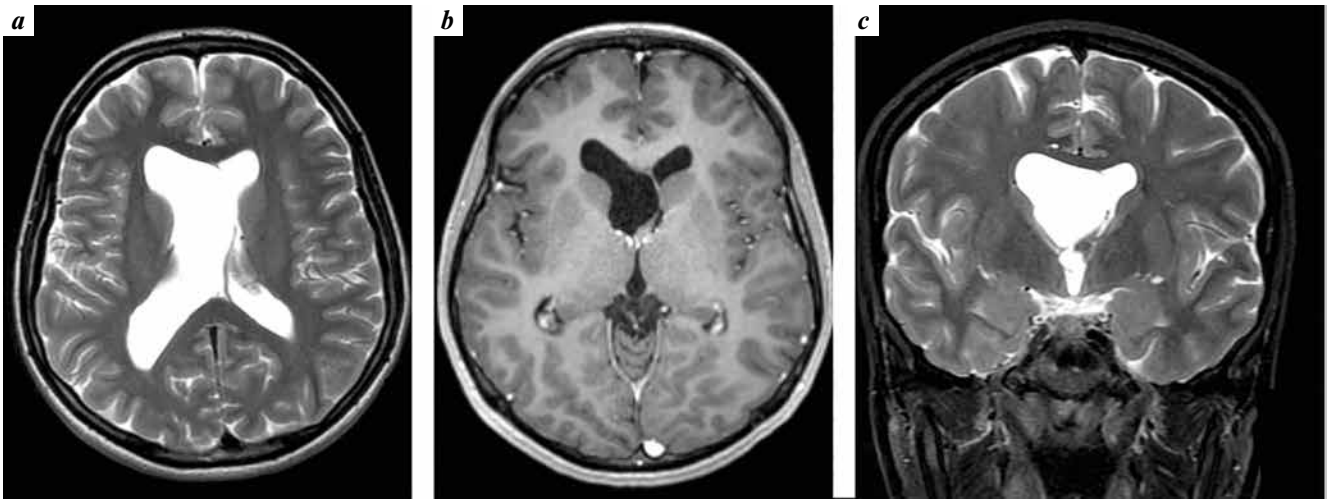

Fig. 1. *Hydrocephalus due to unilateral obstruction of the foramen of Monroe (AH1 D). Axial T2: enlargement of the right lateral ventricle, left dislocation of the septum pellucidum, convexital subarachnoid spaces normal (a). No neoplastic lessions on the post-contrast magnetic resonance imaging (b). Coronal T2: enlargement of the right lateral ventricle, left dislocation of septum pellucidum, membrane obstruction of the right foramen of Monroe (c). The presence of this membrane was confirmed due to endoscopic surgery*

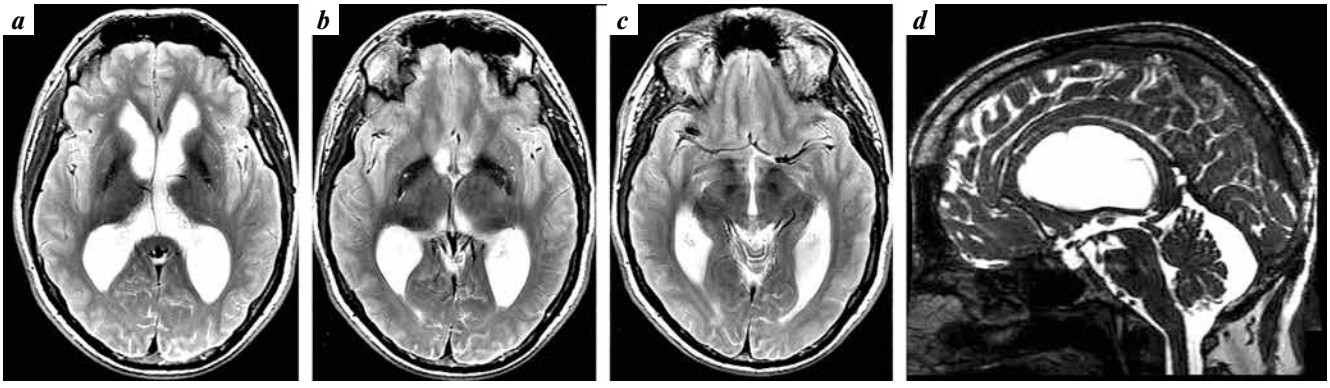

Fig. 2. *Hydrocephalus due to bilateral obstruction of the foramens of Monroe (AH1). Both lateral ventricles are enlarged (a). No neoplastic lesions in the foramens of Monroe (colloid cyst, tumor) (b). Normal size of the 3rd ventricle (c). Sagittal image is demonstrated are flattening of the roof of the 3rd ventricle, 4th ventricle has normal size, subarachnoid spaces of the posterior cranial fossa are normal, aqueduct is free and not enlarged (d)*

intergroup comparison of quantitative parameters, Mann–Whitney test (two-sided variant) was used. Statistically significant level was $p < 0.05$. The results were presented as medians, means, standard deviations, minimums, and maximums.

RESULTS

Among all the forms of AIH, AH2a was the most common. Analysis of age showed that intraventricular obstruction (AH1, AH2a, AH2b) and extraventricular cistern obstruction (AH3) were significantly more frequent in young patients ($p < 0.05$). Mean age in these groups was <60 years. Hydrocephalus with DESH symptom (AH4) can be considered hydrocephalus of the elderly, as mean patient age was 68 ± 6.3 (55–85) years. In cases of AH5 hydrocephalus, no significant correlation with patient age was observed, it occurred equally frequently in all age groups ($p > 0.05$)

In the context of sex, women more frequently developed AH1 (61.5 %) and AH3 (61.5 %) hydrocephalus. For other forms, the ratio between sexes was approximately equal.

Age data and sex distribution for different forms of AIH are presented in Table. 2.

The lateral ventricles were enlarged in all 290 (100 %) patients.

Detailed data on neuroradiological parameters for each AIH type are presented in Table. 3.

Evans, FOHR, FHR and BCR indices values were higher in patients with AH3–0.37 ± 0.06 (0.29–0.64), 0.52 ± ± 0.06 (0.4–0.74), 0.46 ± 0.07 (0.34–0.73), 0.29 ± 0.05 (0.17–0.48), respectively, but only the FOHR parameter was significant ($p = 0.031$).

Enlargement of only one or both lateral ventricles is significantly correlated with type AH1, as well as interventricular septum dislocation and flattening of the roof of the 3rd ventricle ($p < 0.001$). Hydrocephalus types AH2a, AH4 and AH5 were characterized by enlargement of the lateral and 3rd ventricles, while types AH2b, AH3 and some cases of AH4 and AH5 included enlargement of the 4th ventricle.

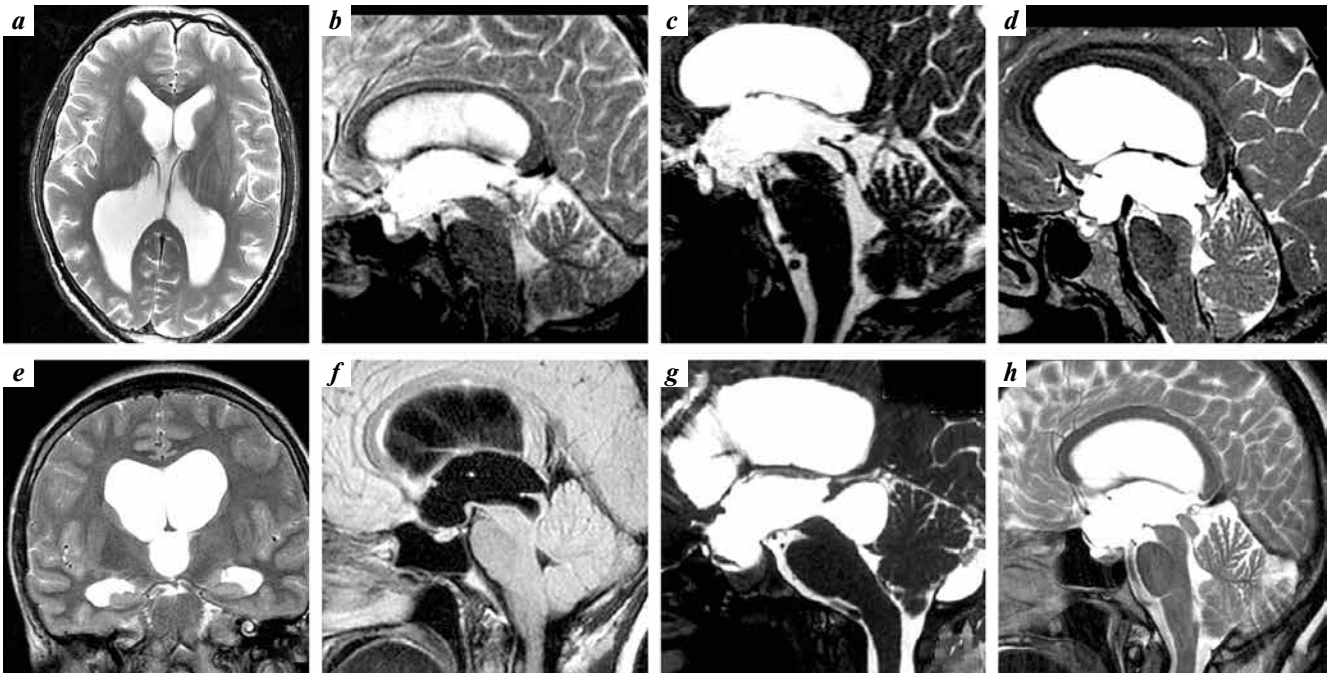

Fig. 3. *Hydrocephalus due to aqueduct stenosis (AH2a): a – axial T2: enlargement of the both lateral ventricles and normal convexital subarachnoid spaces; b – sagittal T2 is making a false impression about patency of aqueduct, frame of the 3rd ventricle is smoothed; c – sagittal FIESTA is verified a membrane of caudal part of the aqueduct; d – typical picture of the obstruction of the aqueduct of brain: lateral ventricles and 3rd ventricle are enlarged, the lumen of the aqueduct is blocked by the membrane, rostral part of the aqueduct is enlarged, premamillary membrane has a ventral position, herniation of tonsillas, compression of the posterior cranial fossa subarachnoid spaces; e – frontal T2 scan: lateral ventricles and 3rd ventricle are enlarged, compression of convexital subarachnoid spaces; f – variant of the aqueduct stenosis with more rostral expansion than on figure "d"; g – sagittal T2 is presented far advanced aqueduct stenosis: whole aqueduct is extremely enlarged as a result of caudal membranous obstruction; h – aqueduct stenosis as a result of thickening of the quadrigeminal plate, T2 signal from this and from the brain are the same, which is making a possible to exclude glioma*

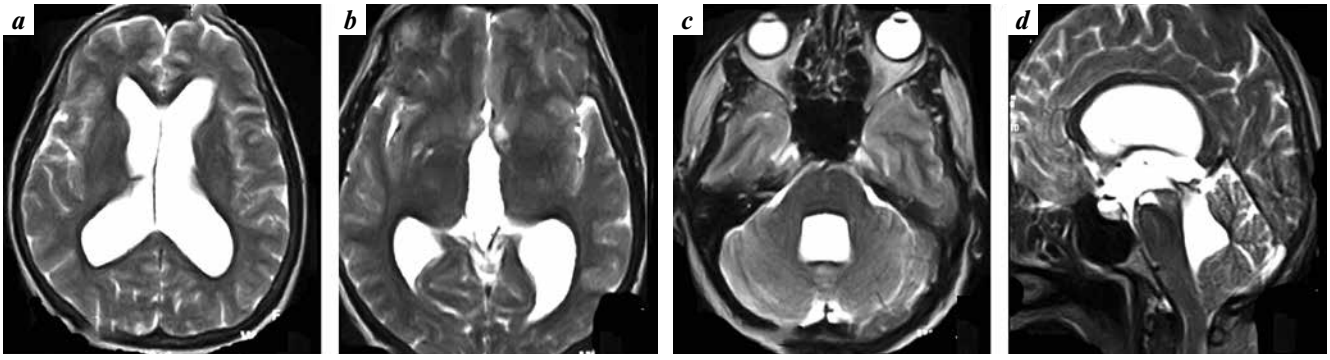

Fig. 4. *Hydrocephalus due to obstruction of the outlets of the 4th ventricle (AH2b): a, b – enlargement of the both lateral and 3rd ventricles, convexital subarachnoid spaces of the posterior cranial fossa are compressed; c – enlargement of the 4th ventricle, convexital subarachnoid spaces of the posterior cranial fossa are compressed; d – sagittal image: ventral dislocation of the premamillary membrane, enlargement of the aqueduct, tonsillas herniation*

Absence of the CSF pulsation artifact in CA is a significant (p <0.001) characteristic only in AH2a type (99.1 %). An exception was seen in 1 patient with incomplete CA stenosis where artifact was preserved but PC-MRI showed signs of CA stenosis.

Type of CA obstruction did not affect selection of surgical treatment tactics. Therefore, frequency of each type was not evaluated.

Presence of a membrane at the exit from the 4th ventricle and absence of CSF pulsation artifact in this area were characteristic of AH2b hydrocephalus (p <0.001). In patients with other types of AIH these features were not observed.

Ventral PMM dislocation was observed in 174 (60 %) patients of the total group. This sign was characteristic of AH2a (85 %), AH2b (100 %) and AH3 (87.7 %) types. The severity of its prolapse wasn»t graded as it did not affect treatment tactics selection.

Convexital SSS was compromised in 118 (40.7 %) patients. Most frequently this symptom was observed in patients

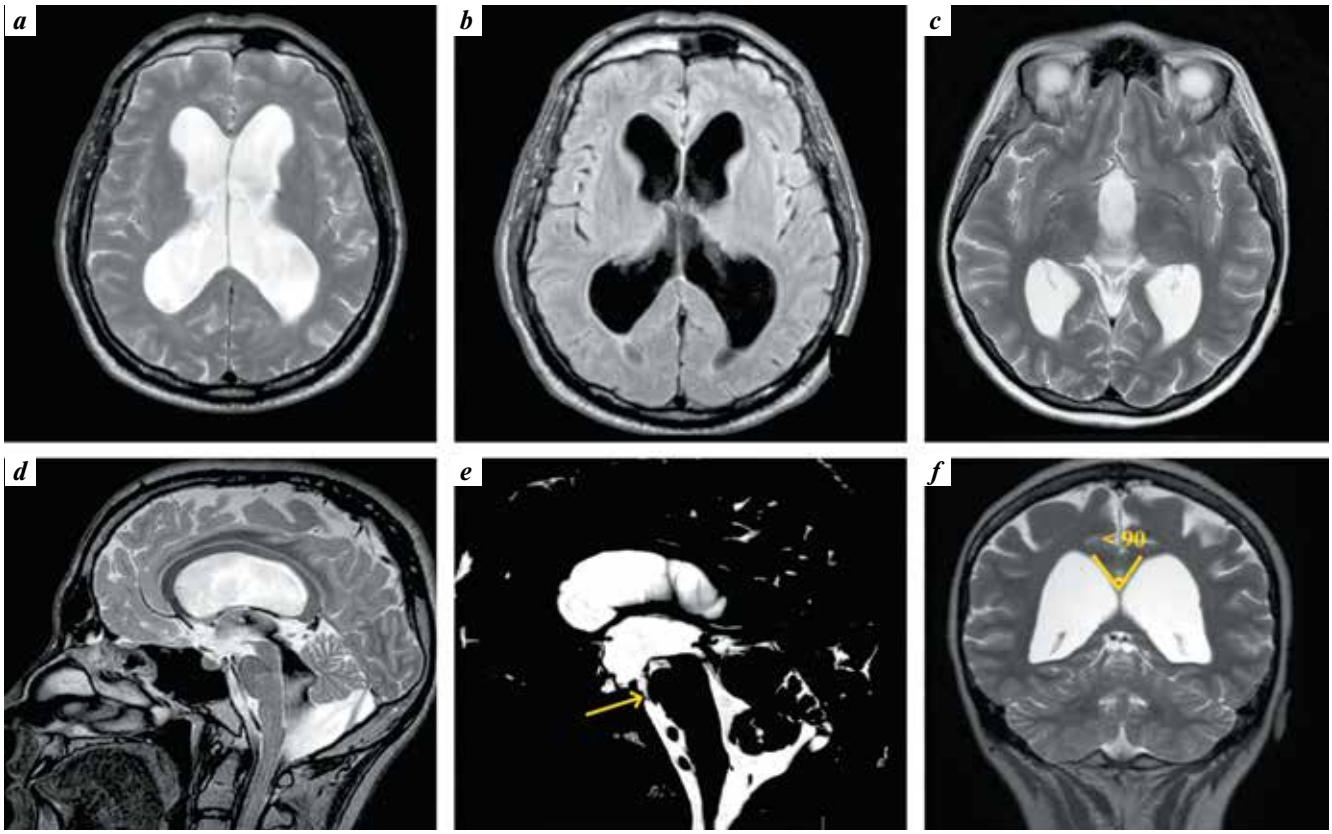

Fig. 5. *Hydrocephalus due to obstruction of the posterior cranial fossa cisterns (AH3). Lateral ventricles and 3rd ventricle are enlarged (a–c), periventricular changing of the signal is absent (a, b), convexital subarachnoid spaces are normal (a, c, f). Sagittal scans are demonstrated, that aqueduct and 4th ventricle outlets are free (d, e). Caudal part of the aqueduct is more expanded than rostral (d, e). Subarachnoid spaces of the posterior cranial fossa are not changed or enlarged (e). Additional membrane between ventral surface of the pons and clivus is visualized on the cisternography scan (arrowed) (e), cisterna magna is enlarged. Corpus collosum corner is sharp (f)*

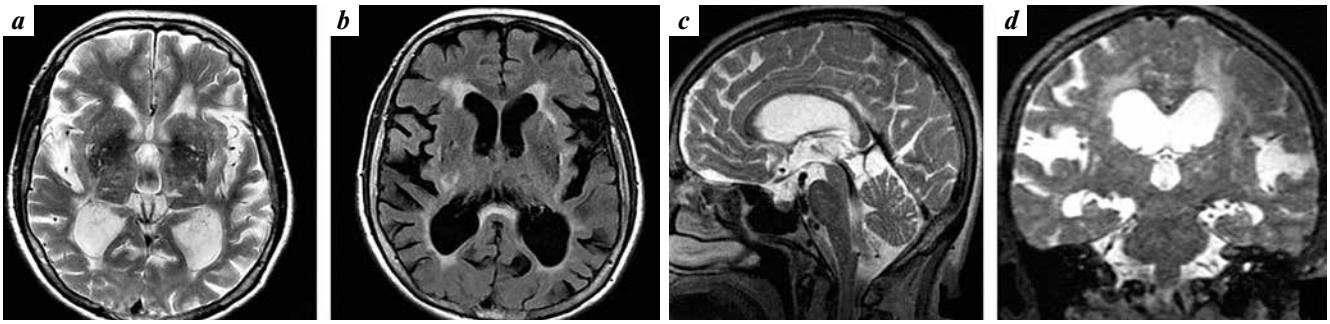

Fig. 6. *Hydrocephalus with DESH-symptom (AH4). Lateral ventricles and 3rd ventricle are enlarged (a, d). Sizes of the 4th ventricle close to normal (c). Premamillary membrane has a normal position, aqueduct and 4th ventricle outlets are free, that's confirmed by the "flow void" on the T2 scan (c). Frontal T2 shows a significant expansion of the lateral fissures, while subarachnoid spaces of the parasaggital and interhemispheric regions are compressed. Hyperintensive periventricular, subcortical and brain stem signal T2 and FLAIR (a, b, d)*

Table 2. *Age and sex difference between different types of idiopathic hydrocephalus of adults*

Parameter	Common group	AH1	AH2a	AH2b	AH3	AH4	AH5
Age, years	50 ± 18.2 (18–85)	40 ± 12.4 (23–67)	42 ± 16.7 (18–77)	47 ± 16.5 (26–74)	46,2 ± 18.1 (18–79)	68 ± 6.3 (55–85)	63 ± 11.8 (29–77)
Sex, %:							
woman	54.1	61.5	49.5	61.1	61.5	48.1	59.3
man	45.9	38.4	50.5	38.9	38.5	51.9	40.7

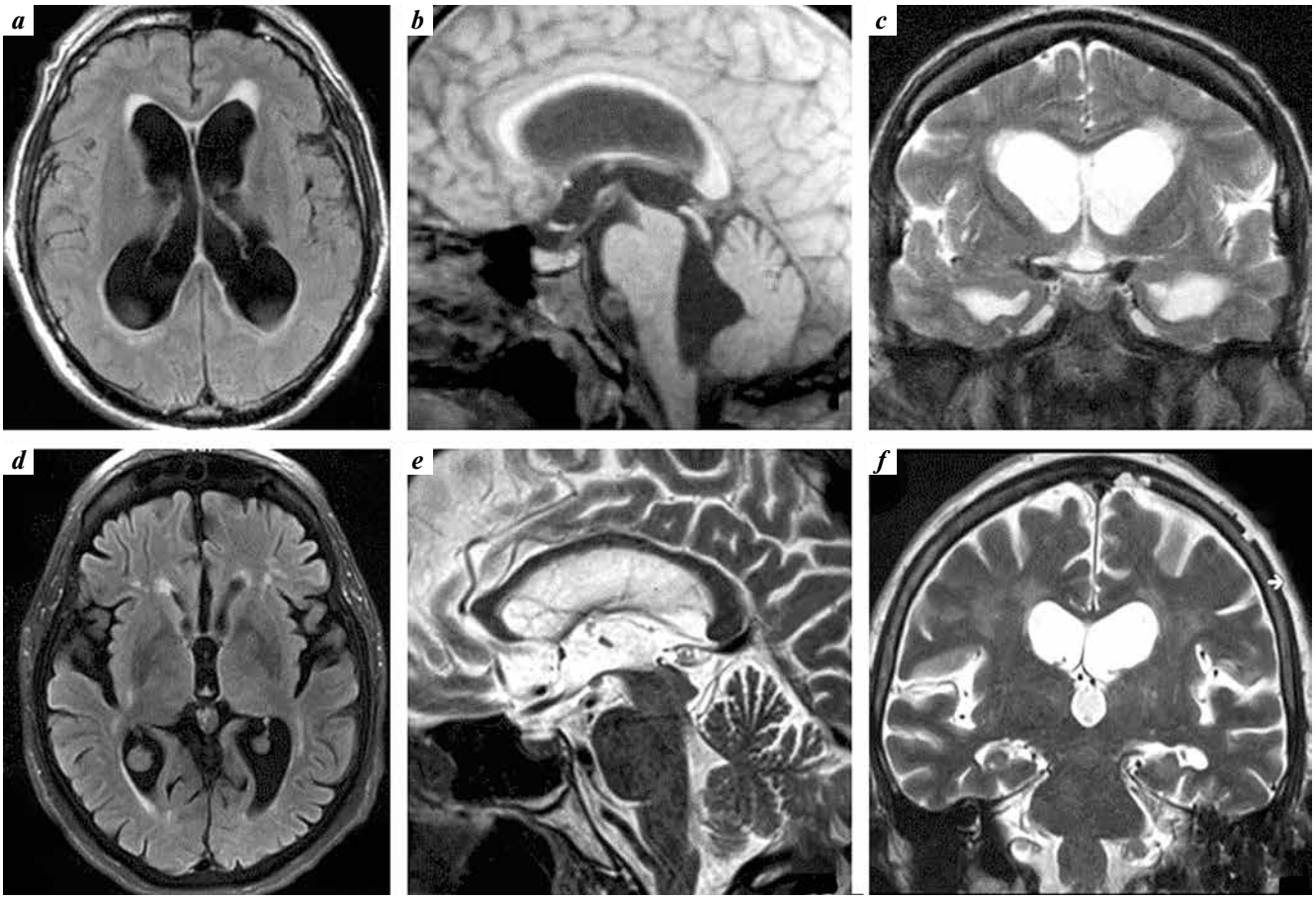

Fig. 7. *Hydrocephalus without verified obstruction (AH5). Scans show a variable of the group of patients AH5. The next signs may be observed at different patients: enlargement of the lateral both (a), 3rd (b, d) and 4th (b) ventricles. Convexital subarachnoid spaces may be compressed (c) or normal (f), or unevenly expanded (f, d). Premamillary membrane has a normal position (b, e). Subarachnoid spaces of the posterior cranial fossa are usual. "Flow void" in the aqueduct (e). Cisterna magna is usual (e). Several foci of hyperintensive signal in T2/FLAIR around ventricles, in the cortex, in the deep white mater of the hemispheres (a, b, d)*

with AH2b (72.3 %) and AH2a (69.9 %) hydrocephalus, and it was never observed in patients with AH4.

DESH symptom was significantly correlated with AH4, «hydrocephalus of the elderly» (p <0.001). In patients aged 60 years and older, DESH was also observed in AH2a (0.9 %).

The 3rd ventricle was enlarged in all patients except the AH1 group. The enlargement was larger in patients with AH2b (p = 0.006) and AH3 (p <0.001).

Enlargement of the 4th ventricle (FVWT and FVWAP) was observed in patients with AH2b (94.4 %), AH3 (89.2 %), as well as in some patients with AH4 (5.5 %) and AH5 (29.6 %). In patients with AH1, the 4th ventricle was always of normal size. Enlargement of the 4th ventricle was significantly associated with AH2b and AH3 (p <0.05).

PCF subarachnoid spaces were enlarged in patients with AH3 (69.2 %) and AH4 (51.9 %) significantly more frequently than in other cases. In contrast, in patients with AH2b a trend toward compression of these CSF spaces was observed (72.2 %) (p = 0.039).

Presence of leukoaraiosis in T2/FLAIR MR images, as well as changes in signal in the basal ganglia, white matter, were significantly more frequent (p <0.001, p = 0.004) in patients with AH4 (96.3 and 87 %, respectively), as well as in other types of intraventricular obstructive hydrocephalus in patients aged 60 years and older.

Increased size of the sella turcica was more common in patients with AH2a and AH2b (33.6 and 33.3 %, respectively), less common in AH3 (21.5 %). In the other groups this sign was minimal or absent.

Cerebral aqueduct was enlarged only rostrally only in patients with AH2a (94.7 %, p <0.001). Separately, enlargement of only the caudal CA was observed in AH3 (73.8 %) and AH2b (11.2 %). Enlargement of CA as a whole was significantly more frequent in AH2b (77.8 %, p = 0.002), and was also seen in AH3 (20 %) and AH5 (3.7 %). CA stenosis with preserved conductance was observed in 1 case only.

Size of the cisterna magna was increased in all patients with AH3 which was a significant sign of this type of AIH (90.8 %, p <0.001).

Table 3. *Radiological parametres in various forms of idiopathic adult hydrocephalus*

Parameter	AH1	AH2a	AH2b	AH3	AH4	AH5	Reference
Index values, M ± SD (min–max)							
Evans	0.3 ± 0.03 (0.26–0.3)	0.36 ± 0.07 (0.24–0.85)	0.35 ± 0.08 (0.25–0.59)	0.37 ± 0.06 (0.29–0.64)	0.34 ± 0.02 (0.27–0.43)	0.34 ± 0.04 (0.25–0.41)	≤0.29
FOHR	0.43 ± 0.05 (0.35–0.57)	0.5 ± 0.06 (0.38–0.7)	0.5 ± 0.08 (0.36–0.66)	**0.52 ± 0.06 (0.4–0.74)** ↑*	**0.44 ± 0.02 (0.38–0.52)** ↓*	0.47 ± 0.06 (0.39–0.68)	–
FHR	0.37 ± 0.03 (0.32–0.42)	0.44 ± 0.08 (0.29–0.87)	0.44 ± 0.1 (0.32–0.68)	0.46 ± 0.07 (0.34–0.73)	0.4 ±0.04 (0.28–0.52)	0.42 ± 0.05 (0.34–0.55)	–
BCR	0.21 ± 0.06 (0.12–0.31)	0.27 ± 0.06 (0.130.69)	0.28 ± 0.07 (0.14–0.39)	0.29 ± 0.05 (0.17–0.48)	0.24 ± 0.02 (0.19–0.33)	0.27 ± 0.04 (0.2–0.37)	–
TVWT	–	0.13 ± 0.02 (0.07–0.23)	0.14 ± 0.04 (0.09–0.22)	0.14 ± 0.02 (0.08–0.24)	0.1 ± 0.01 (0.07–0.16)	0.12 ± 0.02 (0.06–0.2)	–
FVWAP	–	8.44 ± 2.81 (2.5–18.2)	25.3 ± 10.7 (3.3–44)	16.2 ± 4.1 (8–26.8)	12.7 ± 3.1 (6–19.5)	12.3 ± 4.1 (7–22.3)	–
FVWT	–	0.12 ± 0.05 (0.01–0.6)	0.25 ± 0.09 (0.05–0.41)	0.19 ± 0.04 (0.12–0.36)	0.18 ± 0.02 (0.08–0.2)	0.18 ± 0.04 (0.12–0.3)	–
3VSFR	0.54 ± 0.03 (0.48–0.6)	0.5 ± 0.04 (0.31–0.61)	0.5 ± 0.05 (0.39–0.57)	0.48 ± 0.03 (0.41–0.57)	0.45 ± 0.03 (0.41–0.56)	0.46 ± 0.03 (0.41–0.58)	–
Frequency of detection of the sign with the corresponding type of hydrocephalus, %							
Enlargement of lateral ventricles	100	100	100	100	100	100	–
Enlargement of 3rd ventricle	0	100	100	100	100	100	–
Enlargement of 4th ventricle	0	**0** ↓*	**94.4** ↑*	**89.2** ↑*	5.5	29.6	–
Periventricular changes of the signal	33.4	40.7	38.9	18.4	96.3 ↑*	59.2	No
Subcortical and white mater changes of the signal	8.4	8.8	11.1	9.2	**87** ↑*	51.8	No
Pattency aqueduct: free blocked	 100 0	 0.9 99.1	 100 0	 100 0	 100 0	 100 0	Free
Structure of aqueduct: rostral enlargement caudal enlargement enlargement of whole aqueduct narrowed normal	 – – – – 100	 **94.7** ↑* 0 0 1.8 3.5	 0 11.2 **77.8** ↑* 0 0	 0 **73.8** ↑* 20 3.1 0	 0 0 0 0 100	 0 0 3.7 0 96.3	Normal

End of table 3

Parameter	AH1	AH2a	AH2b	AH3	AH4	AH5	Reference
Corner of the corpus callosum by the posterior commissure: <90° >90°	 – –	 76.1 23.9	 83.3 16.7	 89.2 10.8	 98.1 1.9	 81.5 18.5	>90°
Sizes of the sella turcica: enlarged normal	 0 100	 33.6 66.4	 33.3 66.7	 21.5 78.5	 1.9 98.1	 11.1 88.9	Length 9–15 mm Height 7–13 mm
Cisterna magna sizes: normal enlarged	 100 0	 98.2 1.8	 100 0	 9.2 90.8	 100 0	 96.3 3.7	–
SAS PCF: normal enlarged compressed	 91.6 ↑ 0 8.4	 88.5 ↑ 0.9 10.6	 27.8 0 **72.2** ↑*	 27.7 **69.2** ↑* 3.1	 48.1 51.9 0	 63 37 0	Normal
SAS convexital: normal enlarged compressed DESH	 41.7 0 58.3 0	 27.4 **69.9** ↑* 0.9 0.9	 27.7 **72.3** ↑* 0 0	 73.9 ↑ 24.6 1.5 0	 1.9 0 0 **98.1** ↑*	 62.9 7.4 14.8 0	Normal
Position PMM: normal ventral ventral doubtful	 100 0 0	 9.7 **85.8** ↑* 3.5	 0 **100** ↑* 0	 6.1 **87.7** ↑* 4.6	 96.3 **0** ↓* 3.7	 88.9 **0** ↓* 11.1	Normal position
Septum pellucidum: midline lateral	 58.3 **41.7** ↑*	 100 0	 100 0	 100 0	 100 0	 100 0	Midline
Roof of the 3rd ventricle: normal flattened	 58.3 **41.7** ↑*	 100 0	 100 0	 100 0	 100 0	 100 0	Normal
Pattency of the PCF cisterns: saved no	 100 0	 100 0	 100 0	 0 **100** ↑*	 100 0	 100 0	Saved
Tonsillas herniathion	16.7	9.7	**38.8** ↑*	0	0	0	Below Mc Ray line

**p <0.05.*

Note. *The values that statistically significantly (p <0.05) distinguish the corresponding form of hydrocephalus from the rest are highlighted in bold; arrows indicate the direction of statistically significant differences: ↑ – more often or more than with other forms of hydrocephalus; ↓ – less often or less than with other forms of hydrocephalus. SAS – subarachnoid spaces; PCF – posterior cranial fossa; DESH – disproportionally enlarged subarachnoid space hydrocephalus.*

Conductance of the PCF cisterns was preserved in all types except AH3 where it was absent in 100 % of cases. In some patients with AH2b and AH2a, cistern conductance was hard to measure due to strong pressure gradient. Additional membranes in the PCF cisterns were observed only in AH3 which was a pathognomic sign (p <0.001).

Lowering of the cerebellar tonsils into the great occipital foramen was observed in patients with AH1 (16.7 %), AH2a (9.7 %) and AH2b (38.8 %). In other AIH types, dislocation of the cerebellar tonsils did not occur.

DISCUSSION

The etiological factor is one of the main factors in hydrocephalus classification as it determines the advisability of endoscopic operation for correction of CSF flow. Post-infectious, posthemorrhagic, posttraumatic and sometimes congenital hydrocephalus are always associated with abnormal CSF resorption, therefore endoscopic intervention is not effective or useful irrespectively of the presence of intraventricular obstruction. The only approach to treatment for these patients is CSF shunt surgery. Hydrocephalus etiology can be determined through detailed medical history obtained from the patient and their closest circle. Patients with tumors causing CA obstruction that cannot be resected due to various causes, are good candidates for endoscopic 3rd ventriculostomy.

In idiopathic hydrocephalus, identification of the CSF obstruction location, determination of capabilities of endoscopic and shunt surgeries are the basis of quality patient treatment, decreased frequency of complications in the early and late postoperative period.

Detailed knowledge of the anatomy of CSF-containing spaces, sequence of CSF flow in combination with MRI capabilities allow to reasonably accurately verify the level of CSF flow obstruction in the majority of patients [6–11].

The presented classification is relatively simple, logical and includes the whole spectrum of AIH. It is convenient for a surgeon as it allows them to rationally plan invasive pre-surgical diagnostic procedures and helps with treatment method selection.

The presence of hydrocephalus in groups AH1, AH2a, AH2b, AH3 and AH4 is undeniable. Having neuroimaging data, a specialist can focus on the reversibility of the patient's symptoms, probability of further health decline in comparison with the risk of surgical treatment. In AH5 group, due to the absence of reliable data on the presence of CSF flow obstruction, the presence of hydrocephalus is not obvious, and differential diagnosis with diseases accompanied by decreased volume of brain matter due to causes other than abnormal CSF circulation is necessary.

The level of CSF obstruction affects the timing of hydrocephalus progression [5], and this is understandable. In intraventricular obstruction, only transependymal CSF resorption is possible [16]. In obstruction at the basal cistern level, resorption into the lymph vessels along the spinal roots is possible especially in the standing position when CSF pressure in the spinal SSS is maximal. During obstruction only in the convexital SSS, additional resorption occurs in the cranial lymph pathways through the cribriform plate. And in fully conductive SSS, resorption into the interstitial spaces of the brain, as well as venous sinuses through the arachnoid granulations and villi, is available [17]. Considering all these factors, we assume that the classification being discussed allows to deliberately approach the evaluation of the risk of symptom progression in different types of hydrocephalus which affects indications for surgery.

For clarification of indications for hydrocephalus treatment, CSF evaluation is frequently used [18, 19]. In intraventricular obstruction hydrocephalus (AH1, AH2a, AH2b), it is effectively contraindicated. In other cases, it can be performed if indicated.

Predominance of intraventricular obstruction and cistern obstruction in our material can be explained by limited availability of endoscopic equipment. At the same time, CSF shunt surgeries are significantly more accessible. Due to this, the patients were referred to the Neurosurgery Center for consultation.

MRI examination protocol in AIH which we consider to be optimal in the conditions of our clinic is presented in Table 4.

Table 4. *Mandatory magnetic resonance imaging (MRI) components in cases of idiopathic hydrocephalus of adults*

MRI mode	Image projection, comments
T2	Axial, sagittal and coronal
T2 sensitive to CSF pulsing	Sagittal and/or coronal
FLAIR	Axial
Magnetic resonance cisternography (CISS, FIESTA)	Sagittal, coronal
Optional: phase-contrast MRI with cardiosynchronization	Oblique axial scan perpendicular to the aqueduct, quantitative study of the parameters of the CSF pulsing through the aqueduct (necessary if obstruction of the aqueduct is questionable)

Axial T2-weighted and FLAIR images are the standard of survey examination, allowing to assess anatomy of the brain, ventricular system, SSS, presence of periventricular signal changes and other changes in the cerebral parenchyma and propose a possible obstruction level. It is important to have T2-weighted CSF flow-sensitive images [7] which allow to determine conductance of CSF pathways in the narrowest parts of the CSF flow system. In suspected obstruction at the foramen of Monro level, frontal sections are necessary; in all other cases the presence of sagittal images is considered necessary. CSF flow artifact (flow void) is a reliable sign of CSF pathway conductance. In hydrocephalus,

the best anatomical mode is MR cisternography (CISS, 3d-CISS, FIESTA sequences combining high CSF and soft tissue contrast with the absence of artifacts caused by CSF movement allow to visualize the thinnest membranes of the CSF system: in the CA, at the 4th ventricle exit, PCF cisterns) [6, 8, 11, 20]. More accurate data on CSF flow in CA can be obtained using PC-MRI [20, 21] and modern spin labeling techniques (time-SLIP) [21–23]. We consider availability of T2-weighted and MR cisternography images in the corresponding projections entirely sufficient for accurate diagnosis of obstruction location and recommend to use PC-MRI only in cases of suspected incomplete CA stenosis.

The main focus in neuroimaging diagnosis of AIH should be on the number of enlarged ventricles and detection of pressure gradient between different parts of the CSF system. Its detection and possibility of relief are the key to the selection of optimal surgical treatment technique.

Thus, interventricular septum is an anatomical structure which is well visualized in MRI, and its dislocation in either direction testifies to the presence of pressure gradient between the lateral ventricles due to obstruction at the foramen of Monro level on one side. The roof of the 3rd ventricle represented by *tela choroidea* and corpus collosum is also a well-visualized structure which normally has a typical curved upwards position. The concept of normal for these landmarks is relative, it does not have evidence-based digital values, but flattening of these structures and sometimes ventral invagination into the 3rd ventricle in combination with enlargement of both lateral ventricles mean the presence of pressure gradient between them and the 3rd ventricle. This is the rarest type of AIH, and special attention should be paid to differential diagnosis with space-occupying lesions of the foramen of Monro area (primarily, colloid cyst).

PMM dislocation in the ventral direction is the most known and widespread criterion of pressure gradient presence between the ventricular system and cistern of the PCF base. Ventral PMM dislocation is a sign which reliably predicts the effectiveness of endoscopic 3rd ventriculostomy. It consistently occurs in such AIH types as AH2a, AH2b and AH3, and is absent in AH1, AH4, AH5. MR cisternography sagittal images allow to identify additional membranes between the cerebral clivus and stem supporting AH3 type hydrocephalus.

DESH symptom is a peculiar indirect marker of pressure gradient between the different parts of convexital SSS. It is well distinguished in the T2-weighted coronal (frontal) images and reliably points to AH4 hydrocephalus [12, 13].

Such features as intensity of SSS of various locations, cisterna magna, changes in the signal from the cerebral parenchyma, size of the sella turcica, cerebellar tonsils dystopia into the great foramen, ventricular system indices, angle of the corpus collosum and combination of these parameters are additional data indirectly pointing to some level of compensation in intracranial volumetric interactions and disease duration and should be supported by medical history and objective patient examination data.

In our opinion, the main weak point of the presented classification is heterogeneity of the AH5 group. It can include patients: 1) with communicating hydrocephalus of varying nature; 2) AH3 in the compensation stage; 3) encephalopathy of varying origin; 4) neurodegenerative disease. Reliable radiological criteria allowing to distinguish these conditions in routine MRI exams has not yet been determined.

Blitz's classification of hydrocephalus can be used for AIH. It allows to rationally plan further examinations and treatment. Currently, the decision on invasive diagnostics and surgical treatment of patients with AIH should not be made without quality MRI. Otherwise, there exists a high probability of diagnostic errors, unnecessary and/or dangerous surgical manipulations, incorrect selection of treatment tactics and method. The protocol of MRI examination should at minimum include T2-weighted images in the necessary projections, FLAIR in axial plane, MR cisternography (FIESTA/CISS) in sagittal/coronal planes (see Table 4).

CONCLUSION

Study and statistical analysis of MR imaging data allowed to determine general signs occurring in all types of hydrocephalus and specific features characterizing individual types of the disorder. The presented classification is simple, logical, and substantiated, it can be easily applied in neurosurgical and radiological practice and allows to rationally plan diagnostic and treatment measures in patients. The current MRI protocol must at a minimum include T2-weighted and FIESTA/CISS images in the necessary planes, FLAIR images in the axial plane. Other additional imaging studies should be performed for diagnosis specification in ambiguous cases.

REFERENCES

1. Mori K., Shimada J., Kurisaka M. et al. Classification of hydrocephalus and outcome of treatment. Brain Dev 1995;17(5):338–48. DOI: 10.1016/0387-7604(95)00070-r
2. Rekate H.L. The definition and classification of hydrocephalus: a personal recommendation to stimulate debate. Cerebrospinal Fluid Res 2008;5:2. DOI: 10.1186/1743-8454-5-2
3. Dandy W.E. Experimental hydrocephalus. Ann Surg 1919;70(2):129–42. DOI: 10.1097/00000658-191908000-00001
4. Ransohoff J., Shulman K., Fishman R.A. Hydrocephalus: a review of etiology and treatment. J Pediatr 1960;56:499–511. DOI: 10.1016/s0022-3476(60)80193-x
5. Li J., McAllister J.P. 2nd, Shen Y. et al. Communicating hydrocephalus in adult rats with kaolin obstruction of the basal cisterns or the cortical subarachnoid space. Exp Neurol 2008;211(2):351–61. DOI: 10.1016/j.expneurol.2007.12.030
6. Aleman J., Jokura H., Higano S. et al. Value of constructive interference in steady-state three-dimensional, Fourier transformation magnetic resonance imaging for the neuroendoscopic treatment of hydrocephalus and intracranial cysts. Neurosurgery 2001;48(6):1291–5; discussion 1295–6. DOI: 10.1097/00006123-200106000-00021
7. Greitz D. Radiological assessment of hydrocephalus: new theories and implications for therapy. Neurosurg Rev 2004;27(3):145–65; discussion 166–7. DOI: 10.1007/s10143-004-0326-9
8. Laitt R.D., Mallucci C.L., Jaspan T. et al. Constructive interference in steady-state 3D Fourier-transform MRI in the management of hydrocephalus and third ventriculostomy. Neuroradiology 1999;41(2):117–23. DOI: 10.1007/s002340050715
9. Dlouhy B.J., Capuano A.W., Madhavan K. et al. Preoperative third ventricular bowing as a predictor of endoscopic third ventriculostomy success. J Neurosurg Pediatr 2012;9(2):182–90. DOI: 10.3171/2011.11.PEDS11495
10. Kehler U., Gliemroth J. Extraventricular intracisternal obstructive hydrocephalus – a hypothesis to explain successful 3rd ventriculostomy in communicating hydrocephalus. Pediatr Neurosurg 2003;38(2):98–101. DOI: 10.1159/000068053
11. Dinçer A., Kohan S., Ozek M.M. Is all "communicating" hydrocephalus really communicating? Prospective study on the value of 3D-constructive interference in steady state sequence at 3T. AJNR Am J Neuroradiol 2009;30(10):1898–906. DOI: 10.3174/ajnr.A1726
12. Kitagaki H., Mori E., Ishii K. et al. CSF spaces in idiopathic normal pressure hydrocephalus: morphology and volumetry. AJNR Am J Neuroradiol 1998;19(7):1277–84.
13. Hashimoto M., Ishikawa M., Mori E. et al. Diagnosis of idiopathic normal pressure hydrocephalus is supported by MRI-based scheme: a prospective cohort study. Cerebrospinal Fluid Res 2010;7:18. DOI: 10.1186/1743-8454-7-18
14. Mori E., Ishikawa M., Kato T. et al. Guidelines for management of idiopathic normal pressure hydrocephalus: second edition. Neurol Med Chir (Tokyo) 2012;52(11):775–809. DOI: 10.2176/nmc.52.775
15. O'Hayon B.B., Drake J.M., Ossip M.G. et al. Frontal and occipital horn ratio: a linear estimate of ventricular size for multiple imaging modalities in pediatric hydrocephalus. Pediatr Neurosurg 1998;29(5):245–9. DOI: 10.1159/000028730
16. Bloch O., Auguste K.I., Manley G.T., Verkman A.S. Accelerated progression of kaolin-induced hydrocephalus in aquaporin-4-deficient mice. J Cereb Blood Flow Metab 2006;26(12):1527–37. DOI: 10.1038/sj.jcbfm.9600306
17. Pollay M. The function and structure of the cerebrospinal fluid outflow system. Cerebrospinal Fluid Res 2010;7:9. DOI: 10.1186/1743-8454-7-9
18. Relkin N., Marmarou A., Klinge P. et al. Diagnosing idiopathic normal-pressure hydrocephalus. Neurosurgery 2005;57 (3 Suppl): S4–16; discussion ii–v. DOI: 10.1227/01.neu.0000168185.29659.c5
19. Bergsneider M., Miller C., Vespa P.M., Hu X. Surgical management of adult hudrocephalus. Neurosurgery 2008;62(Suppl 2):643–59; discussion 659–60. DOI: 10.1227/01.neu.0000316269.824667.f7
20. Ucar M., Guryildirim M., Tokgoz N. et al. Evaluation of aqueductal patency in patients with hydrocephalus: three-dimensional high-sampling-efficiency technique (SPACE) *versus* two-dimensional turbo spin echo at 3 Tesla. Korean J Radiol 2014;15(6):827–35. DOI: 10.3348/kjr.2014.15.6.827
21. Luetmer P.H., Huston J., Friedman J.A. et al. Measurement of cerebrospinal fluid flow at the cerebral aqueduct by use of phase-contrast magnetic resonance imaging: technique validation and utility in diagnosing idiopathic normal pressure hydrocephalus. Neurosurgery 2002;50(3):534–43; discussion 543–4. DOI: 10.1097/00006123-200203000-00020
22. Bradley W.G. Jr., Scalzo D., Queralt J. et al. Normal-pressure hydrocephalus: evaluation with cerebrospinal fluid flow measurements at MR imaging. Radiology 1996;198(2):523–9. DOI: 10.1148/radiology.198.2.8596861
23. Yamada S., Miyazaki M., Kanazawa H. et al. Visualization of cerebrospinal fluid movement with spin labeling at MR imaging: preliminary results in normal and pathophysiologic conditions. Radiology 2008;249(2):644–52. DOI: 10.1148/radiol.2492071985

Authors' contributions
K.V. Shevchenko: research design development, data collection, analysis and interpretation, article writing;
V.N. Shimansky, S.V. Tanyashin: research design development, editing of the article;
V.K. Poshataev, V.V. Karnaukhov: collecting data for analysis;
M.V. Kolycheva: data collection, editing of the article;
K.D. Solozhentseva: data collection and interpretation;
Yu.V. Strunina: statistical data processing.

ORCID of authors
K.V. Shevchenko: https://orcid.org/0000-0003-3732-6664
V.N. Shimansky: https://orcid.org/0000-0002-3816-847X
S.V. Tanyashin: https://orcid.org/0000-0001-8351-5074
V.K. Poshataev: https://orcid.org/0000-0002-3279-3733
V.V. Karnaukhov: https://orcid.org/0000-0002-2581-8648
M.V. Kolycheva: https://orcid.org/0000-0002-7741-6616
K.D. Solozhentseva: https://orcid.org/0000-0001-9984-9327
Yu.V. Strunina: https://orcid.org/0000-0001-5010-6661

Conflict of interest. The authors declare no conflict of interest.

Funding. The study was performed without external funding.

Compliance with patient rights and principles of bioethics. The article presents anonymized patient data.

Article submitted: 12.04.2022. **Accepted for publication:** 13.06.2023.